Appendix of A Large-scale Annotated Mechanical Components Benchmark for Classification and Retrieval Tasks with Deep Neural Networks

Sangpil Kim*[1], Hyung-gun Chi*[1], Xiao Hu[1], Qixing Huang[2], and Karthik Ramani[1]

[1] Purdue University
[2] The University of Texas at Austin
{kim2030, chi45, hu440, ramani}@purdue.edu
huangqx@cs.utexas.edu

1 Statistics of dataset B

Dataset B is aggregated 3D mechanical components from 3D Warehouse*** and GrabCAD†. The labels of dataset B do not follow the hierarchical taxonomy of MCB dataset. When creating the dataset A, we re-annotated and re-arranged each class of dataset B to merge with the data from TraceParts‡, based on International Classification for Standards (ICS [1]). dataset B has total number of 18,038 models with 25 classes. A detailed statistics of the dataset is listed in Table 1.

Table 1. The statistics of dataset B.

Class	# Models	Class	# Models
Bearings	1,117	Nuts	1,069
Bushes	592	Pins	2,659
Castors	1,109	Plates	366
Clamps	157	Pullies	312
Discs	109	Rings	551
Fittings	1,756	Rivets	51
Flanges	398	Rotors	470
Fork joints	47	Screws	3,661
Gears	515	Springs	348
Handles	1,751	Studs	352
Hinges	61	Switches	177
Hooks	122	Washers	880
Motors	746	**Total**	**18,038**

* These authors made an equal contribution.
*** https://3dwarehouse.sketchup.com/
† https://grabcad.com/
‡ https://www.traceparts.com/

2 Experiments on only aligned data

We built Dataset C as aggregated data from only TraceParts which are all aligned. Then, we benchmarked classification and retrieval tasks with seven networks.

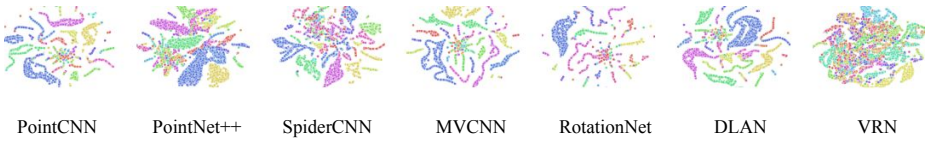

Fig. 1. T-SNE [6] plots of seven different deep neural networks trained with Dataset C. We set perplexity as 40 and iterate 300 times.

2.1 Retrieval benchmark

Table 2. Summary table of evaluation metrics of shape retrieval benchmark for seven deep learning methods. They are grouped by their representation types. Each *, †, and ⊠ symbol indicates the method point cloud, volumetric, and image, respectively.

Method	micro					macro				
	P@N	R@N	F1@N	mAP	NDCG@N	P@N	R@N	F1@N	mAP	DCG@N
PointCNN* [5]	0.912	0.912	0.689	0.901	0.923	0.860	0.802	0.826	0.880	0.845
PointNet++* [7]	0.870	0.870	0.666	0.872	0.862	0.834	0.773	0.796	0.862	0.817
SpiderCNN* [9]	0.908	0.908	0.703	0.922	0.881	0.883	0.809	0.833	0.906	0.857
MVCNN⊠ [8]	0.516	0.516	0.431	0.585	0.436	0.547	0.481	0.498	0.635	0.545
RotationNet⊠ [4]	0.756	0.756	0.63	0.836	0.618	0.813	0.701	0.722	0.851	0.760
DLAN† [3]	**0.952**	**0.952**	**0.719**	**0.941**	**0.961**	**0.919**	**0.866**	**0.891**	**0.927**	**0.903**
VRN† [2]	0.755	0.755	0.588	0.777	0.716	0.708	0.61	0.63	0.771	0.676

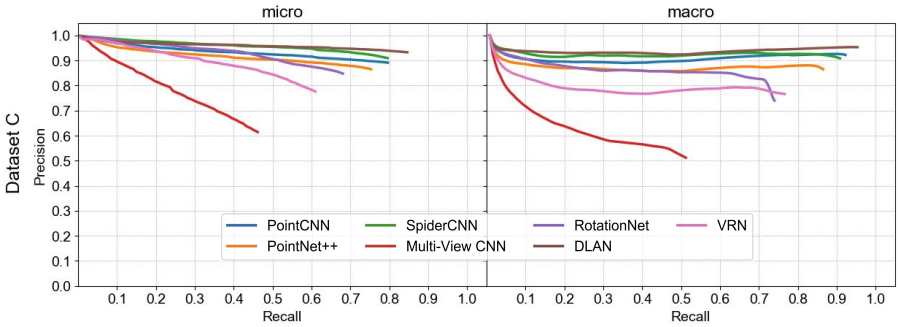

Fig. 2. Precision-recall curve plots for retrieval benchmark with seven different methods. The DLAN shows the best retrieval results.

2.2 Classification benchmark

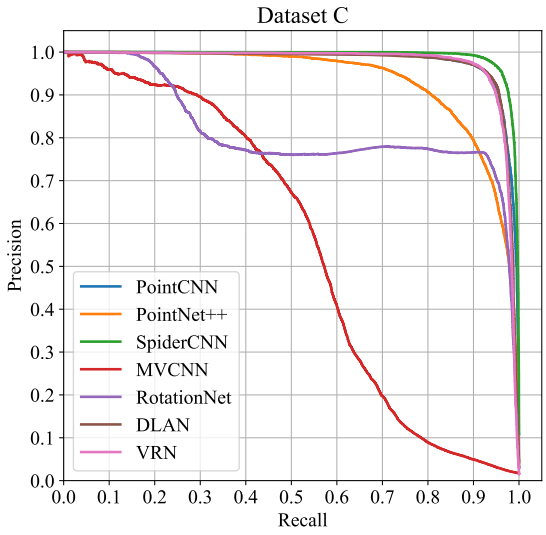

Fig. 3. Precision and Recall curve plots of classification task. The RotationNet shows the best performance in terms of accuracy.

Table 3. Benchmark results of the seven classification models which were trained and evaluated on our mechanical engineering part benchmark. We trained five times per model and reported the highest result. Each *, †, and ⊠ symbol indicates the method: point cloud, volumetric, and image representation, respectively.

Method	Acc. over object (%)	Acc. over class (%)	F1-score	Average Precision
PointCNN* [5]	93.77	71.91	74.46	83.70
PointNet++* [7]	89.97	78.82	78.48	79.45
SpiderCNN* [9]	95.68	80.97	82.12	88.78
MVCNN⊠ [8]	61.29	76.71	62.20	69.38
RotationNet⊠ [4]	96.08	82.61	84.75	80.47
DLAN† [3]	93.99	83.82	83.43	87.17
VRN† [2]	93.47	74.37	74.35	80.68

3 Density Distribution of Classification Results

We plot the probability density distribution of classification results of the Dataset A to clarify the inconsistency between PR curve and accuracy. In the Figure 4, 5, positive states the samples of one class, and all other samples are assigned to negative. Density distributions of positive and negative in RotationNet [4](Figure 4) are separated but closer than VRN [2](Figure 5) which explains the dropping of PR curve of classification task. Other networks that show high classification accuracy and a good PR curve have similar density distribution as VRN.

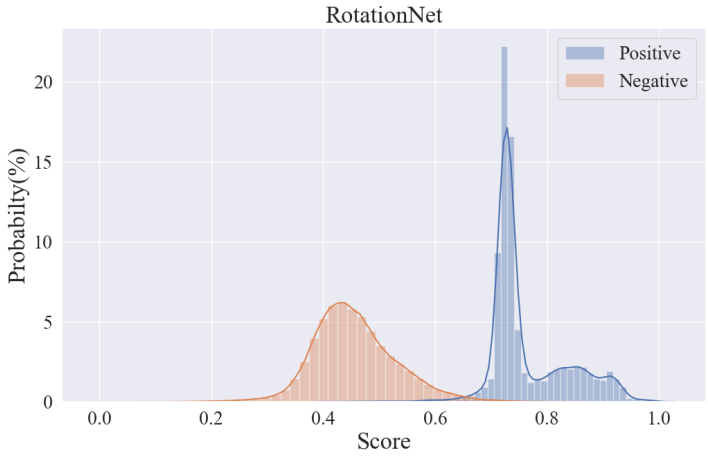

Fig. 4. Probability density distribution of classification results of RotationNet.

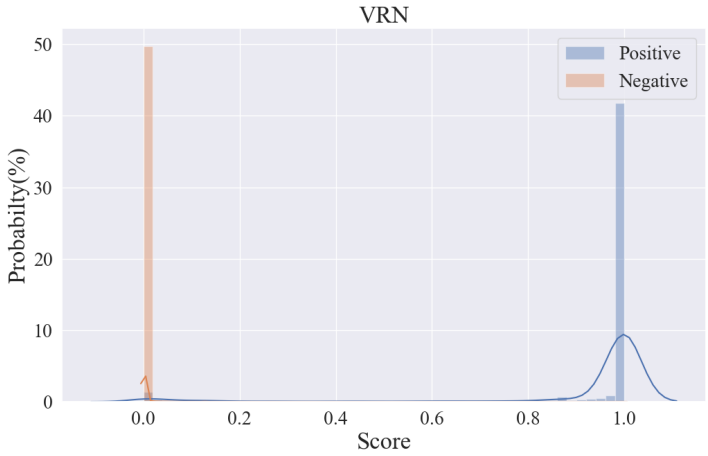

Fig. 5. Probability density distribution of classification results from VRN.

4 Detail information of the retrieval benchmark

Figure 7 shows the hierarchical taxonomy of Mechanical Components Benchmark (MCB). We provide confusion matrix plot of seven methods [2–5,7–9] to visualize the details of classification results on Figure 8 and 9. The accuracy of individual class of each method on both datasets A and B are listed in Table 4 and 5. The representative mechanical objects are shown in Figure 10. The retrieval results are depicted in Figure 6.

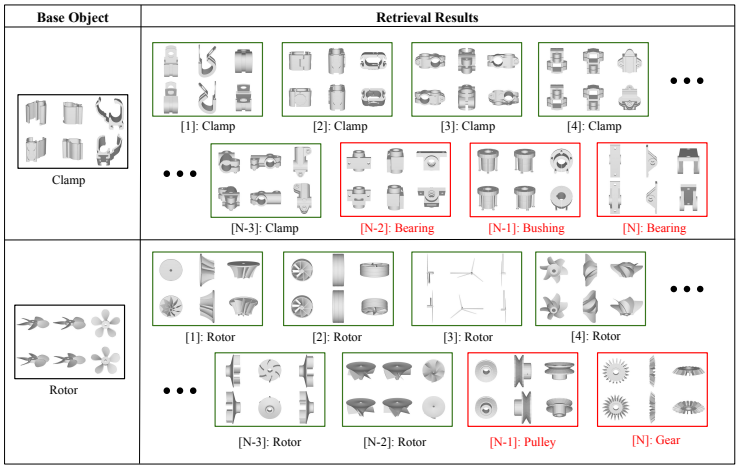

Fig. 6. Sample retrieval results of category Clamp and Rotor. N is the number of data in the corresponding class of the query. Within the first N retrievals, green-border images represent the true positive results, and red-border images represent the false positive results.

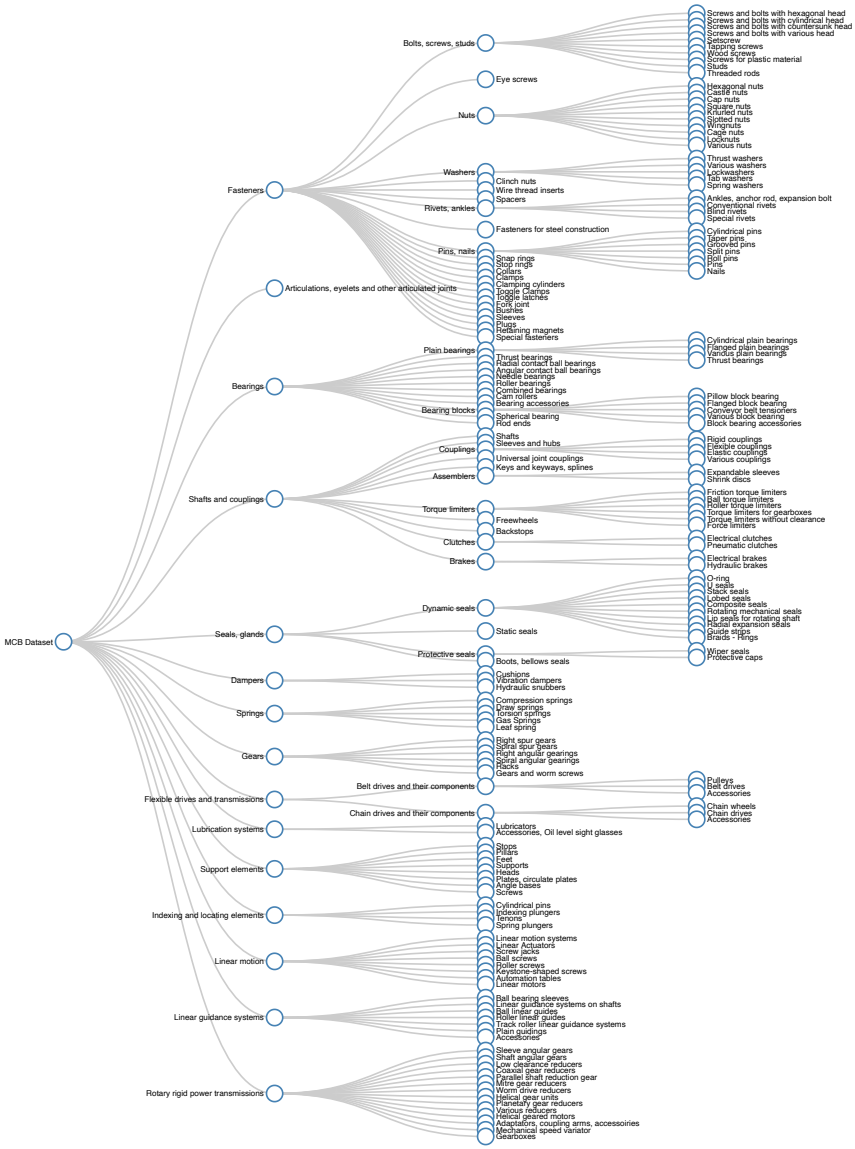

Fig. 7. The hierarchy taxonomy of mechanical components which are based on the International Classification for Standards (ICS).

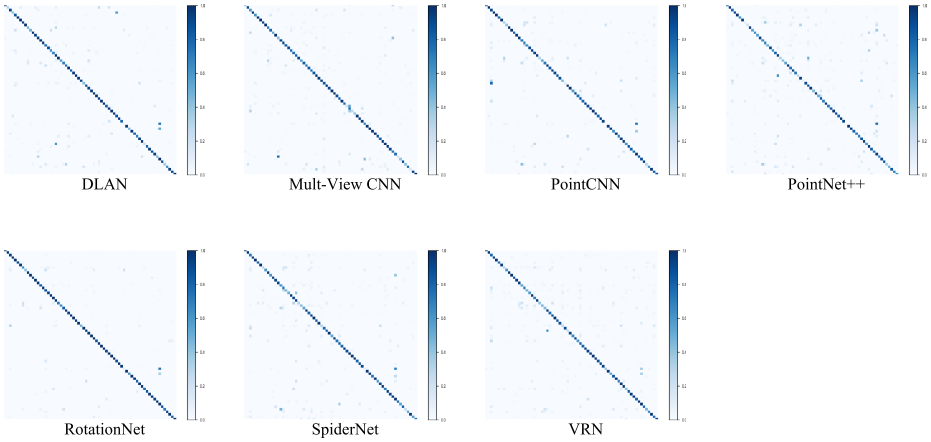

Fig. 8. Confusion Matrix of seven different deep neural networks trained with the dataset A.

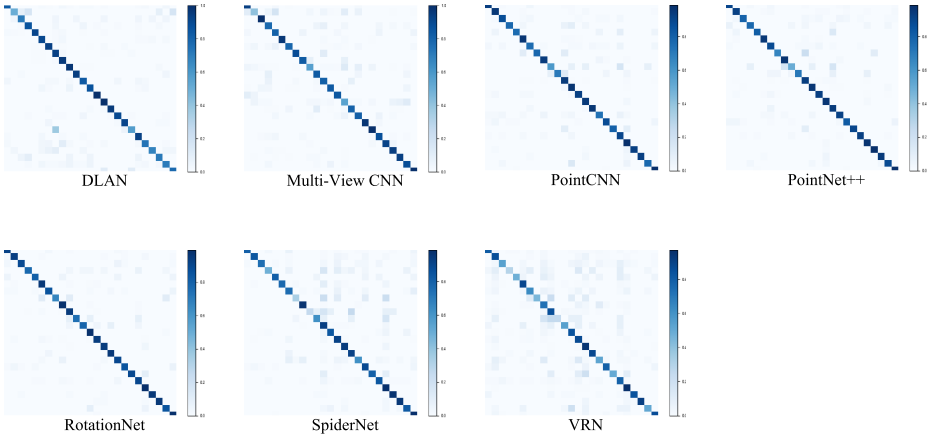

Fig. 9. Confusion Matrix of seven different deep neural networks trained with the dataset B.

Fig. 10. Samples of Mechanical Components Benchmark (MCB) dataset of a total 68 classes.

Table 4. Classification results of dataset A for seven different benchmark and 68 classes.

Class	Point CNN	Point Net++	Spider Net	Multi-View CNN	Rotation Net	DLAN	VRN
Articulations eyelets & joints	0.988	0.880	1.000	0.452	1.000	0.964	0.997
Bearing accessories	1.000	1.000	1.000	0.917	1.000	0.333	1.000
Bushes	0.914	0.776	0.722	0.580	0.947	0.929	0.789
Cap nuts	0.978	0.911	0.933	1.000	1.000	0.429	0.911
Castle nuts	1.000	1.000	1.000	0.618	1.000	0.862	1.000
Castor	0.789	0.632	0.789	0.978	0.895	1.000	0.737
Chain drives	1.000	0.950	1.000	1.000	1.000	1.000	0.950
Clamps	0.355	0.097	0.290	0.947	0.645	0.947	0.323
Collars	0.400	0.200	0.600	1.000	0.400	1.000	0.600
Conventional rivets	0.993	0.974	1.000	0.710	0.999	0.484	0.986
Convex washer	1.000	0.556	0.611	0.800	1.000	0.500	1.000
Cylindrical pins	0.813	0.633	0.960	0.543	0.908	0.993	0.863
Elbow fitting	0.961	0.566	0.920	1.000	1.000	0.944	0.974
Eye screws	0.965	0.947	0.942	0.449	0.987	0.953	0.960
Fan	0.738	0.667	0.619	0.921	0.833	0.987	0.548
Flanged block bearing	0.688	0.688	0.734	0.912	1.000	0.969	0.700
Flanged plain bearings	0.636	0.500	0.455	0.857	0.875	0.762	0.488
Flange nut	0.900	0.900	0.500	0.900	0.909	0.900	0.591
Grooved pins	0.967	0.644	0.967	0.788	0.996	0.625	1.000
Helical geared motors	0.938	0.808	0.903	0.773	0.986	0.682	0.699
Hexagonal nuts	0.981	0.942	0.952	0.808	0.986	0.966	0.971
Hinge	0.300	0.300	0.300	0.889	0.700	0.981	0.400
Hook	0.565	0.435	0.435	0.600	0.652	0.600	0.478
Impeller	0.724	0.552	0.536	0.826	0.828	0.696	0.448
Keys and keyways, splines	1.000	0.991	1.000	0.750	1.000	0.759	1.000
Knob	0.847	0.756	0.817	0.848	0.931	1.000	0.771
Lever	0.966	0.922	0.946	0.771	0.990	0.824	0.888
Locating pins	0.909	0.727	1.000	0.845	1.000	0.961	1.000
Locknuts	0.860	0.280	0.840	1.000	0.940	1.000	0.860
Lockwashers	0.895	0.953	0.977	0.960	1.000	0.980	0.884
Nozzle	0.467	0.067	0.333	0.953	0.500	0.919	0.300
Plain guidings	0.111	0.889	0.778	0.833	1.000	0.433	0.889
Plates, circulate plates	0.973	0.877	0.822	1.000	0.986	0.889	0.288
Plugs	1.000	0.970	1.000	0.918	0.970	0.945	0.939
Pulleys	0.583	0.458	0.542	1.000	1.000	0.970	0.667
Radial contact ball bearings	0.967	0.967	0.954	1.000	0.987	0.958	0.950
Right angular gearings	0.750	0.500	0.750	0.891	0.833	0.987	0.583
Right spur gears	0.886	0.852	0.862	0.830	1.000	0.932	0.841
Rivet nut	0.800	0.700	0.800	1.000	1.000	1.000	0.800
Roll pins	0.997	0.975	0.997	0.799	0.997	0.981	0.984
Screws and bolts with countersunk head	0.886	0.716	0.880	0.182	0.908	0.804	0.941
Screws and bolts with cylindrical head	0.985	0.877	0.989	0.720	0.995	0.995	0.970
Screws and bolts with hexagonal head	0.999	0.984	0.990	0.266	0.998	0.980	0.979
Setscrew	0.981	0.917	0.989	0.436	0.992	0.992	0.985
Slotted nuts	0.800	0.800	0.800	1.000	0.867	0.867	0.867
Snap rings	0.950	0.983	0.926	0.950	1.000	0.992	0.909
Socket	0.953	0.924	0.930	0.959	0.971	0.784	0.924
Spacers	0.000	0.000	0.091	0.682	0.091	0.045	0.409
Split pins	0.968	0.979	0.968	1.000	0.979	0.979	0.979
Springs	0.938	0.954	0.969	1.000	0.636	0.455	0.545
Spring washers	0.636	0.818	0.727	0.969	1.000	0.985	0.862
Square	1.000	0.714	1.000	1.000	1.000	0.786	1.000

Square nuts	0.700	0.700	0.600	0.900	0.800	0.700	0.700
Standard fitting	0.947	0.875	0.887	0.803	0.993	0.954	0.967
Studs	0.985	0.935	0.987	0.962	0.996	0.968	0.994
Switch	0.618	0.588	0.706	0.971	0.765	0.235	0.412
Taper pins	0.875	0.958	0.964	1.000	0.850	0.800	0.850
Tapping screws	0.823	0.826	0.906	0.940	0.970	0.970	0.970
Threaded rods	0.760	0.721	0.971	0.735	1.000	0.880	0.972
Thrust washers	0.989	0.961	0.989	0.796	0.911	0.961	0.814
T-nut	0.850	0.700	0.800	0.196	1.000	0.475	0.961
Toothed	0.889	0.889	0.556	0.416	0.996	0.996	0.994
T-shape fitting	0.925	0.851	0.836	0.889	0.889	0.889	0.778
Turbine	0.294	0.353	0.235	0.412	0.706	0.353	0.471
Valve	0.611	0.500	0.556	0.778	0.944	0.667	0.667
Washer bolt	0.978	0.852	0.989	0.159	0.989	0.951	0.989
Wheel	0.813	0.688	0.604	0.938	0.813	0.917	0.771
Wingnuts	0.900	0.600	0.700	1.000	1.000	1.000	0.900
Bearings	0.923	0.885	0.808	0.946	0.923	0.904	0.808
Bushes	0.966	0.915	0.839	0.403	0.941	0.737	0.856

Table 5. Classification results of dataset B for seven different benchmark and 25 classes.

Class	Point CNN	Point Net++	Spider Net	Multi-View CNN	Rotation Net	DLAN	VRN
Castors	0.875	0.819	0.750	1.000	0.889	0.931	0.542
Clamps	0.806	0.806	0.484	0.758	0.871	0.677	0.290
Discs	0.762	0.762	0.810	0.810	0.810	0.714	0.476
Fittings	0.963	0.957	0.778	0.967	0.957	0.960	0.883
Flanges	0.747	0.911	0.769	0.785	0.861	0.709	0.633
Fork joints	0.667	0.667	0.333	0.889	0.667	0.778	0.444
Gears	0.922	0.961	0.971	0.833	0.990	0.902	0.725
Handles	0.937	0.943	0.929	0.558	0.946	0.914	0.857
Hinges	0.667	0.583	0.250	0.875	0.833	0.500	0.250
Hooks	0.708	0.667	0.625	0.812	0.792	0.708	0.542
Motors	0.973	0.973	0.839	0.859	0.980	0.933	0.839
Nuts	0.930	0.925	0.916	0.850	0.893	0.841	0.869
Pins	0.951	0.970	0.943	0.560	0.955	0.930	0.945
Plates	0.945	0.945	0.918	0.822	0.959	0.945	0.877
Pullies	0.754	0.918	0.617	0.792	0.902	0.836	0.525
Rings	0.900	0.827	0.890	0.987	0.845	0.864	0.791
Rivets	0.800	0.900	0.800	1.000	0.900	1.000	0.500
Rotors	0.892	0.935	0.839	0.889	0.892	0.86	0.785
Screws	0.985	0.981	0.985	0.911	0.992	0.996	0.971
Springs	0.942	0.986	0.971	0.949	0.971	0.957	0.841
Studs	0.929	0.943	0.957	0.943	0.971	0.914	0.914
Switches	0.771	0.886	0.829	0.871	0.914	0.571	0.514
Washers	0.983	0.989	0.989	1.000	0.989	0.971	0.863

References

1. International Classification for Standards. ISO, 7 edn. (2015)
2. Brock, A., Lim, T., Ritchie, J.M., Weston, N.: Generative and discriminative voxel modeling with convolutional neural networks. arXiv preprint arXiv:1608.04236 (2016)
3. Furuya, T., Ohbuchi, R.: Diffusion-on-manifold aggregation of local features for shape-based 3d model retrieval. In: Proceedings of the 5th ACM on International Conference on Multimedia Retrieval. pp. 171–178. ACM (2015)
4. Kanezaki, A., Matsushita, Y., Nishida, Y.: Rotationnet: Joint object categorization and pose estimation using multiviews from unsupervised viewpoints. In: Proceedings of the IEEE Conference on Computer Vision and Pattern Recognition. pp. 5010–5019 (2018)
5. Li, Y., Bu, R., Sun, M., Wu, W., Di, X., Chen, B.: Pointcnn: Convolution on x-transformed points. In: Advances in Neural Information Processing Systems. pp. 820–830 (2018)
6. Maaten, L.v.d., Hinton, G.: Visualizing data using t-sne. Journal of machine learning research **9**(Nov), 2579–2605 (2008)
7. Qi, C.R., Yi, L., Su, H., Guibas, L.J.: Pointnet++: Deep hierarchical feature learning on point sets in a metric space. In: Advances in neural information processing systems. pp. 5099–5108 (2017)
8. Su, J.C., Gadelha, M., Wang, R., Maji, S.: A deeper look at 3d shape classifiers. In: Proceedings of the European Conference on Computer Vision (ECCV). pp. 0–0 (2018)
9. Xu, Y., Fan, T., Xu, M., Zeng, L., Qiao, Y.: Spidercnn: Deep learning on point sets with parameterized convolutional filters. In: Proceedings of the European Conference on Computer Vision (ECCV). pp. 87–102 (2018)